

# Quadruped Robot with Tensegrity Joints actuated via Pneumatic Artificial Muscles

Antoine Vincent Martin, Jan Petrs, Alexander Dittrich, Dario Floreano

**Abstract**—The design of a quadruped robot with tensegrity joints and McKibbens artificial muscles is a complex challenge, as it involves the intricate task of designing a multi-axis compliant joint integrated with compliant actuation. Analytical resolutions, simulations, and real-world measurement were necessary to solve this complex design problem. The demonstrator itself was first tested in Mujoco simulation before actually building it.

It was possible to eliminate the need for antagonistic pairs of muscles thanks to the introduction of a restoring force in every joint, hence reducing by a factor of two the number of actuators when compared with the antagonistic approach, eventually making the robot lighter. The pneumatic actuators are controlled by onboard valves and a microcontroller. The tensegrity joints are an assembly of 3d printed thermoplastic polyurethane and 3d printed PETG.

Thanks to the joints' restoring force, the quadruped has the ability to stand by itself without active actuator control. This follows the idea of a compliant quadruped robot with minimal sensory feedback. So far, the robot has been shown to be capable of walking forward in simulation and on a flat surface with the demonstrator (while being supported by a rail).

**Index Terms**—Tensegrity, Pneumatic Artificial Muscles, McKibbens, Soft Actuator, Quadruped Robot, Reinforcement Learning

## I. INTRODUCTION

### Tensegrity joints and Pneumatic Artificial Muscles Motivations

For a robot to steadily walk, it is necessary for it to adapt to its environment, i.e. the robot must comply with its surrounding ([1, Actuators research, p.10]). This behaviour would also make the quadruped inherently safer for humans.

Optimally, compliant joints should be actuated with compliant actuators. Compliant actuators can be extrinsic or intrinsic. The extrinsic one denotes any system requiring an active feedback loop to simulate this compliancy (e.g. impedance control). On the other hand, the intrinsic one uses passive systems (e.g. springs), it is on this later sort of compliancy this project will be based upon. In fact, it requires less demanding control (fewer sensors) when compared to its extrinsic counterpart.

Tensegrity structures can be inherently compliant. The ratio  $\frac{\text{free DOF's stiffness}}{\text{blocked DOF's stiffness}}$  can be tuned to have various degree of omnidirectional compliance. Such joints are then capable to deform to absorb impact (see [1, Structure Design, p.12]).

Tensegrity joints can also be used to store energy in order to have elastic energy cycling or restoration force. In the case of a robot using actuators producing work only when in contraction or only in extension, the prevalent theory suggests the usage of antagonistic pairs of muscle (see Birdbot [2]). However,



Fig. 3: Quadruped Robot

some animals like the guinea fowl (a terrestrial bird) and some robots (BirdBot [2]) are able to walk even without antagonistic pairs of muscle. Instead, restoring forces provided by tendon and spring mechanism are used. There are many benefits from using such system:

- Robot/Animal have intrinsic stability, it is able to stand without providing energy
- If constrained to use only contractive actuators (e.g. McKibbens), then only half the number of actuators are needed when compared to antagonistic pairs of muscles.

Tensegrity and more generally compliant joints are also more robust against harsh environments (reduced wear, reduced maintenance) when compared with regular rigid linking mechanism (see [3]).

Robots like the StarETH quadruped robot ([4]) implemented this concept using series elastic actuator (SEA)-driven articulated leg (see [1, Articulated legs, p.5]). SEA uses springs to introduce compliance even if using high reduction ratio gears (or anti-backlash actuators), therefore making the actuators capable to withstand shocks. Furthermore, the blocking properties of the actuators in SEA can be used to be in stance phase without applying torque on actuators.

This compliancy can also be implemented on hydraulic actuator (see [5]). But this technology was not used here,

The authors are with the Laboratory of Intelligent Systems, Ecole Polytechnique Federale de Lausanne (EPFL), CH1015 Lausanne, Switzerland.

since this project is about intrinsic compliancy. Out of all the actuators featuring intrinsic compliancy, McKibben are the actuators which have the best balance between ease of control (at least for a binary control), ease of manufacturing, weight, range of achievable force and strain, and cost ([6, Fluidic soft actuators, p. 236]).

### Related Work

The domain of tensegrity is vast, many joints have already been imagined, build, and proven in real world (see [7]).

The tensegrity joint developed here is based upon the work of Erik Mortensen ([8]). This leg features compliant joints as well as compliant actuators, using the SEA concept ([1, Articulated legs, p.5]). The level of impedance can be modulated using a tertiary actuator (stepper motor) located in the limb, which vary the level of pretension in the SEA's spring. However, the actuators (2 servo-motor + 1 stepper motor) are embedded into the leg's limb. In addition, the servomotors are too slow, which makes this leg not suited for agile gait and makes it hard to harness the possibility of energy cycling coming with the tensegrity joints. This joint featured an actuated range of motion of nearly 180° and was suited for cable driven actuation. However, the joints for this quadruped do not need such range and even though it can enter the *cable driven category*, the actuators will not be embedded into the limbs. A new joint must be therefore developed (see II-B).

Replacing the servo with McKibben would greatly benefit the performance of the leg (increase the agility of the joint, off-loading the limb). Even though quadruped driven with McKibben is not a new concept (and it was proven as a viable actuation method, see [9]), to the extent of my knowledge, no tensegrity-joint based quadruped robot with McKibben actuators was ever constructed.

This brings to the subject of this project, designing a quadruped robot with compliant joint using tensegrity and compliant actuators using McKibbens.

## II. METHODS

### A. Quadruped topology

The initial decision in the design process was to determine the kind of quadruped robot to be developed. The final decision was to design a mammal-type quadruped robot (its counterpart being the sprawling-type). Mammal-type legs are prone to smaller joint torque than sprawling-type leg ([1, Articulated legs, p.3]), therefore increasing the maximum load. It was also decided to design the quadruped for forward walking gait on flat terrains only. Thus, rendering redundant the roll DOF of the hip joint (i.e. each leg will only have 2 actuated DOFs).

The quadruped must feature intrinsic stability (i.e. must stand by itself without any active control loop). To do so, the joints must be stiff enough to support the quadruped's weight, but not too much to avoid over loading the actuators.

The way the tensegrity based hinge are constructed (flexible thermoplastic used in combination with 3d printing) makes them difficult to model their stiffness. As a result, joint stiffness is only evaluated through experimentation, which makes it challenging to conduct more than a few iterations.

Therefore, for the sake of simplicity, an important design choice was made: all joints will feature the same stiffness.

One effect of such decision is lateral foot displacement when a vertical force is applied (e.g. weight of the robot), see the shift  $\Delta f$  in fig 4. This shift  $\Delta f$  pushes the center of mass closer to the boundary of the support polygon, which is bad for the stability. It is however possible to mitigate this shift by arranging the leg in a  $><$  configuration (instead of  $<<$ ), see fig 6.

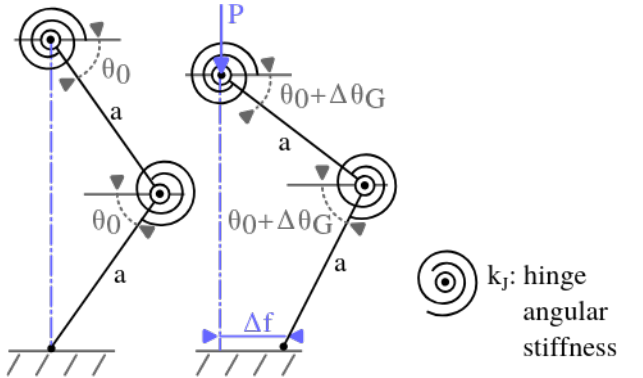


Fig. 4: Effect of weight on hinge's angles

By conducting an energy analysis on a single leg, one can determine the joint stiffness for a specific angle deflection  $\Delta\theta_G$ . The weight applied to the hip is considered to be the fourth of the total quadruped mass. The energy before the robot is released (i.e. no moment applied on the hinge, the feet are at an infinitesimal distance from the ground) should equal the energy at equilibrium. The limb weights are ignored (small mass when compared to the trunk mass)

$$\frac{2amg}{4} \sin(\theta_0) = \frac{2amg}{4} \sin(\theta_0 - \Delta\theta_G) + 2 \frac{1}{2} k_J \Delta\theta_G^2 \\ \implies k_J = \frac{amg}{2\Delta\theta_G^2} (\sin(\theta_0) - \sin(\theta_0 - \Delta\theta_G))$$

$\Delta f$  can be estimated using trigonometry:

$$\Delta f = a \cdot [\cos(\theta - \Delta\theta) + \cos(2\theta)]$$

The following assumptions are made:

- $m = 1.5kg$  total mass of the trunk
- $\theta_0 = 60^\circ$  natural stance yet not too close to singularity point
- $\Delta\theta_G = 20^\circ$  deflection caused by the gravity
- $a = 30cm$  limb length, between hip and knee

The resulting angular joint stiffness is equal to  $k_J \approx 4Nm$  and the lateral foot displacement  $\Delta f \approx 8cm$ .

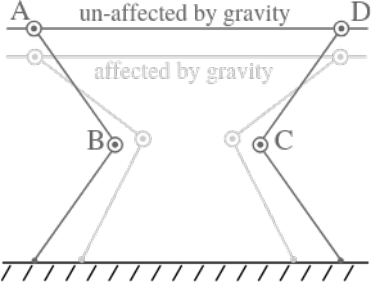


Fig. 5: Effect of gravity when not actuated

### B. Tensegrity Joint choice

The requirements for the new joints are:

- actuated range of motion:  $\approx 45^\circ$
- omnidirectional compliance
- stiffness:  $\approx 4Nm$
- simple design, easy to manufacture

The iterative nature of designing such a joint led to numerous designs, some with 3D printed elastic tendons (TPU), others with cable and pre-tensioning mechanism. Different geometry were tested as well. The final iteration is described in section III-C.

### C. Walking Policy

The quadruped features fast actuation and elastic energy storage capability. It is therefore suited for dynamic walking gait. The quadruped platform does not have any sensors (except in simulation where a 6 degrees IMU is used to estimate roll, pitch and 3 axis speeds and accelerations). Since the quadruped cannot sense the joint space, the walking gaits will have to be open loop.

This project does not focus on the quadruped walking gait. However, as a proof of concept that the quadruped topology is worthy of walking, a virtual clone was build using the Mujoco environment. This part was crucial for this project as it gave deep insight about the quadruped without yet having a real model.

In order to quickly iterate through designs, a Python program was written, automatically generating the required *.xml* description of the quadruped used by the Mujoco simulator. The Python script was used to quickly generate different configurations (such as muscle attachment point, joint's angle, limb length, quadruped mass, e.t.c.). It is then possible to simulate the effect of those parameters within Mujoco.

This simulator was crucial for understanding in depth the robot, discover unsuspected behaviours and simulate tensegrity structures (see fig 7).

## III. RESULTS

### A. McKibben Characterization

The length and stiffness of McKibben actuators change with pressure. For a given pressure, the stiffness is pretty much linear (see fig 8), for this reason, a McKibben artificial muscle can be modelled as a linear (see [10]) spring characterized

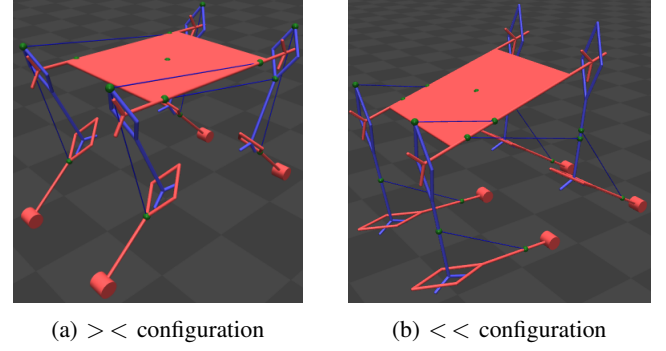


Fig. 6: Different quadruped configurations inside Mujoco

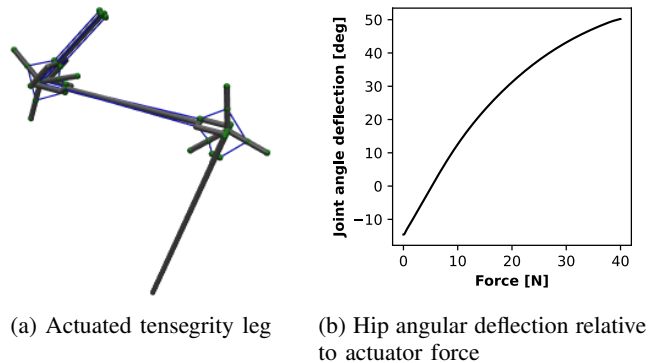


Fig. 7: Tensegrity in Mujoco, simulating hip (the upper joint) joint's angular deflection relative to actuator force, actuator is modelled with the artificial muscle actuator type.

by 2 pressure dependent quantities:  $k_p$  and  $n_p$ . For each pressure, the stiffness  $k_p$  was extracted from fig 8) with a linear regression. The strain at rest coefficient  $n_p$  is the relative difference between the length when inflated and the the length when deflated.

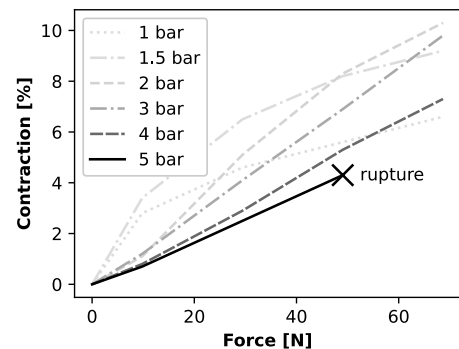


Fig. 8: Contraction over Force, measured with a weighing hook, manually recording the strain and force

When implementing a McKibben, one should choose the operating pressure, and then use the corresponding normalized stiffness and strain (see fig 9).

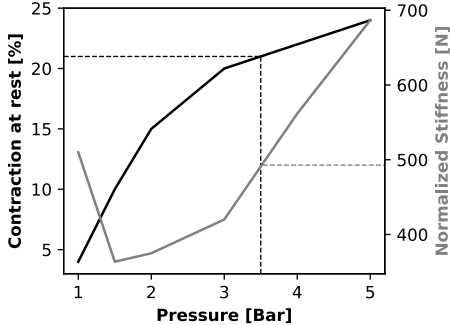


Fig. 9: Operating point of a McKibben muscle, for a given pressure (e.g. a pressure of 3.5 bar implies a 21% contraction ratio at rest and a normalized stiffness of 490N)

The stiffness at low pressure (1 bar and below) is higher to stiffness of higher pressure. In fact, at near atmospheric pressure, the inflation is very low, thus the stiffness mainly comes from the McKibben mesh (which is stiff). Around pressures of 2 to 3 bars, the pressure is high enough such that it inflates the muscle. However, the pressure is still too low for it to provide high stiffness. It is only at 4 bar and above that the stiffness induced by inflating surpasses the stiffness at atmospheric pressure.

The stiffness  $k_p$  can be expressed in terms of the normalized stiffness:  $k_p = \frac{E(p) \cdot A(p)}{l_0}$ , the normalized stiffness is the Young modulus times the cross-section area.  $E A_p$  is used as the symbol to denote this quantity, with  $p$  specifying the operating pressure.

Finally, for a muscle rest length (no load, no pressure)  $l_0$ , the force required to reach a muscle length of  $l$  at operating pressure  $p$  is:

$$\frac{EA_p}{l_0} (l - l_0 \cdot (1 - n_p)) \quad (1)$$

### B. Actuator Dimensioning

McKibben requires some considerations about where to attach its two end in order to achieve the desired performance. (for each joint, the muscle should deflect the joint angle by  $\Delta\beta = 20^\circ$ ). Two approach were taken to meet the displacement requirement:

- empirical muscle placement for joint A, B and C (see fig 5)
- analytical muscle placement for joint D

The joint D (see fig 5) starts from the rest angle  $\theta = -40^\circ$  (i.e. position at rest when considering gravity,  $-60^\circ$  without gravity). The figure 10b illustrates the modelled system, with the horizontal limb grounded (grounding the other side of the side doesn't make any difference).

The joint itself features an angular stiffness  $k_J = 4N/m$  as determined in II-A.

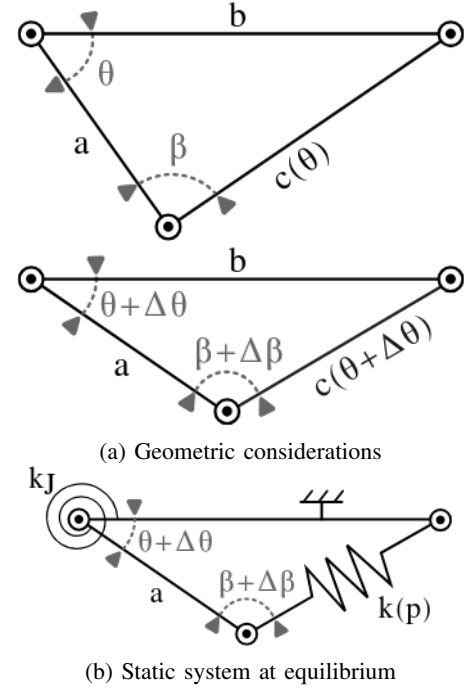


Fig. 10: Joint's system

Considering the static system (no acceleration at equilibrium point), the 2<sup>nd</sup> law of Newton tells us:

$$k_J \Delta\theta = k_p (c(\theta + \Delta\theta) - c(\theta)(1 - n_p)) \cdot a \cdot \sin(\beta + \Delta\beta) \quad (2)$$

With the sine law:

$$a \cdot \sin(\beta + \Delta\beta) = \frac{ab}{c(\theta + \Delta\theta)} \sin(\theta + \Delta\theta) \quad (3)$$

Substituting the McKibben stiffness and using the cosine law, the system equation is:

$$\left\{ \begin{array}{l} c(\theta) = \sqrt{a^2 + b^2 - 2 \cdot ab \cdot \sin(\theta)} \\ c(\theta + \Delta\theta) = \sqrt{a^2 + b^2 - 2 \cdot ab \cdot \sin(\theta + \Delta\theta)} \end{array} \right. \quad (4)$$

$$\left\{ \begin{array}{l} c(\theta + \Delta\theta) = \sqrt{a^2 + b^2 - 2 \cdot ab \cdot \sin(\theta + \Delta\theta)} \\ \frac{k_J \Delta\theta}{EA_p \sin(\theta + \Delta\theta)} = ab \frac{c(\theta + \Delta\theta) - c(\theta)(1 - n_p)}{c(\theta)c(\theta + \Delta\theta)} \end{array} \right. \quad (5)$$

$$\left\{ \begin{array}{l} \frac{k_J \Delta\theta}{EA_p \sin(\theta + \Delta\theta)} = ab \frac{c(\theta + \Delta\theta) - c(\theta)(1 - n_p)}{c(\theta)c(\theta + \Delta\theta)} \end{array} \right. \quad (6)$$

This system can be reduced to one equation, but it is split into 3 parts for the sake of clarity.

All the terms on the left-hand side of the equation 6 are known, leaving only  $a$  and  $b$  as free parameters (see fig 10a for lengths and angles definition).

This system can be solved numerically, producing the results shown on figure 12.

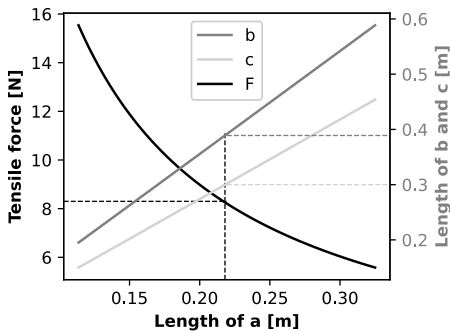


Fig. 12: Length **b**, **c** and force **F** for a given length **a**

The design of the quadruped imposes some constraints:

$$a \in [0.1, 0.3]m$$

$$b < 0.5m$$

$$F < 50N : \text{max load before muscle failing (see fig 8)}$$

The final demonstrator have  $a = 21.8\text{ cm}$ , which accordingly to fig 12 implies a length  $b = 38.9\text{ cm}$ , a length  $c = 30\text{cm}$ , and a max tensile force in the muscle of  $8.3\text{N}$ .

### C. Tensegrity Joint design

The final iteration (fig 11a) checks all the requirements described in the section II-B. It is made of 2 kind of elastic tendons, for a total of 5 tendons. The first 3 tendons' main purpose is linking, whereas the last 2 tendons' purpose is to stiffen the joint.

The tendons are made out of NinjaFlex® TPU (Thermoplastic polyurethane) 3D printed on Prusa 3D printers.

It is possible to set 6 different base angles (one every  $60^\circ$ , see fig 11c) by varying the linking tendons' stacking order (in blue in figure 11b).

You can find some of the discarded iterations in the appendix B.

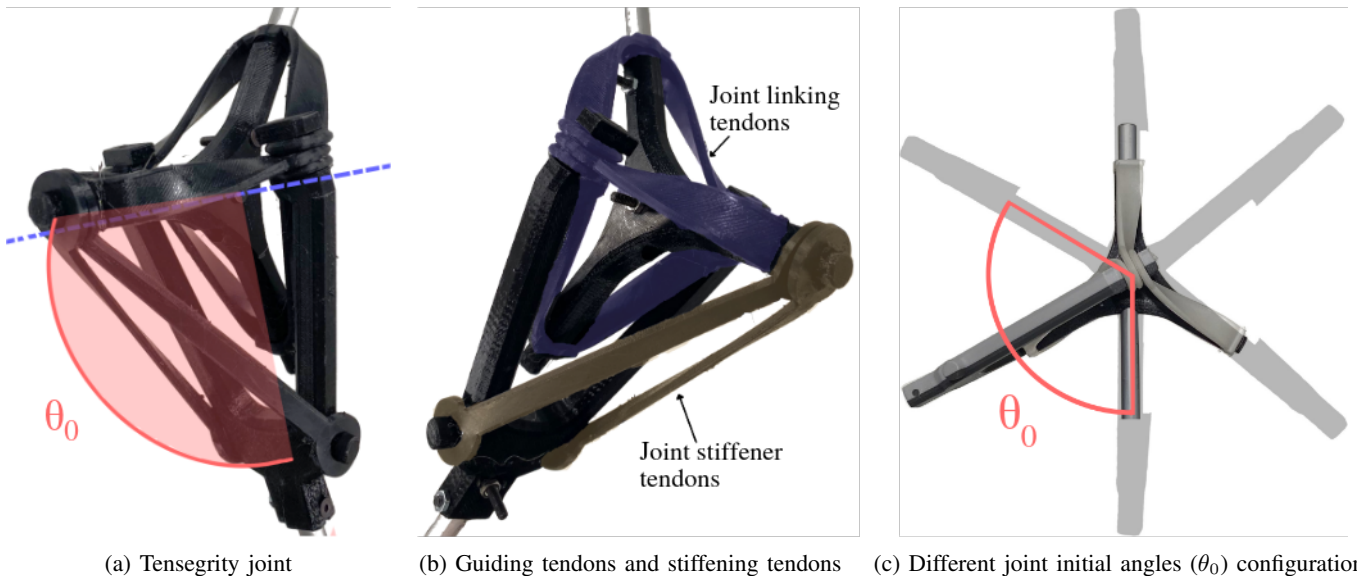


Fig. 11: Tensegrity joint

### D. Pneumatic Network and Electronic

The pneumatic valve used (*SMC vdw250-5g-2-01f-q*) features 3 ports, the McKibben is connected to the IN Port (Input), the pressurized air supply is connected to N.O. port (Normally Open) and is used to inflate the muscle. The N.C. port (Normally Closed) is used to release to the atmosphere the pressure inside the McKibben (see fig 13).

As there are 8 McKibben, a total of 8 pneumatic valves is required. They can be operated with a 24V DC signal, therefore requiring power switches (simple common emitter circuit using TIP122) activated by the MCU (see the appendix A for more details).

The working pressure is around 3.5 bar. This pressure is high enough such that the McKibbens can make the joints bend, and it is low enough to avoid excessive leakage in the valves.

The pressure and the 24V DC power supply are provided via a tethered cable

The topology of the pneumatic network forces the actuator to be either inflated or deflated, with no option for partial inflate. Using proportional valves instead could lead to smoother gait, however it requires more complex control, and they are more expensive.

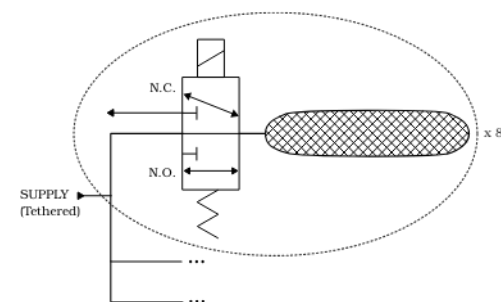


Fig. 13: Pneumatic network schematic

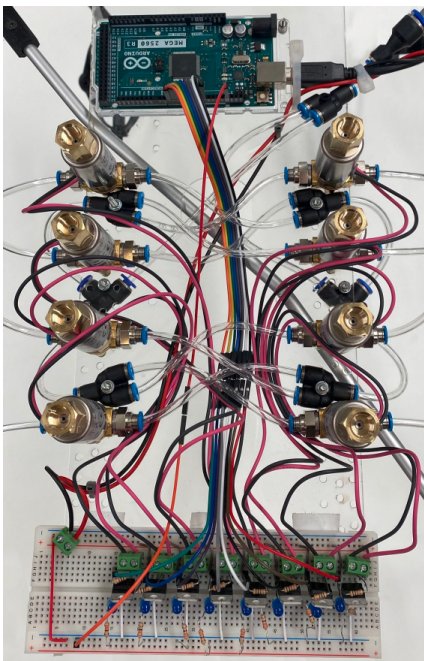
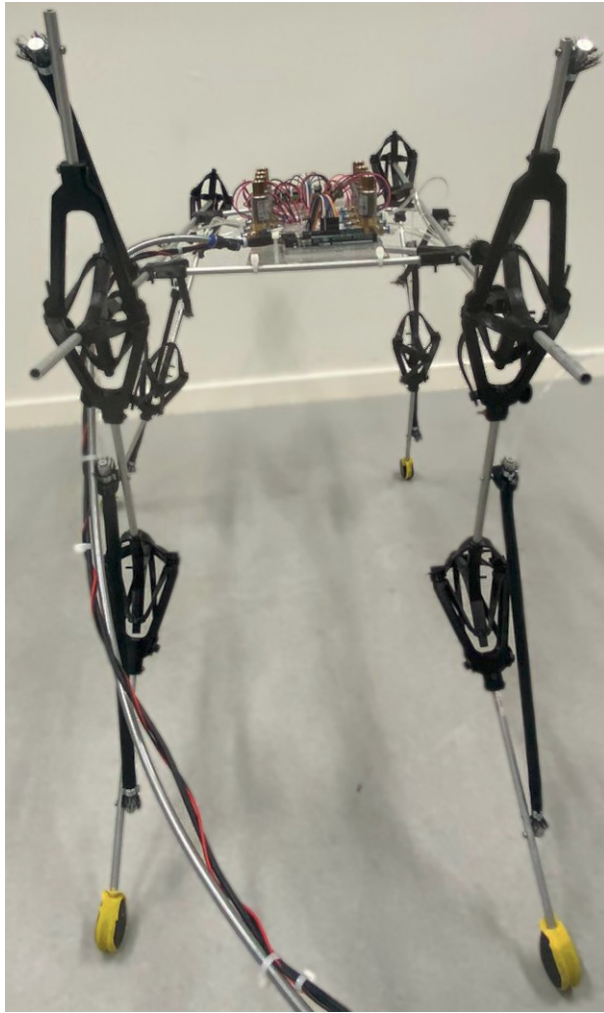


Fig. 15: Demonstrator's controller



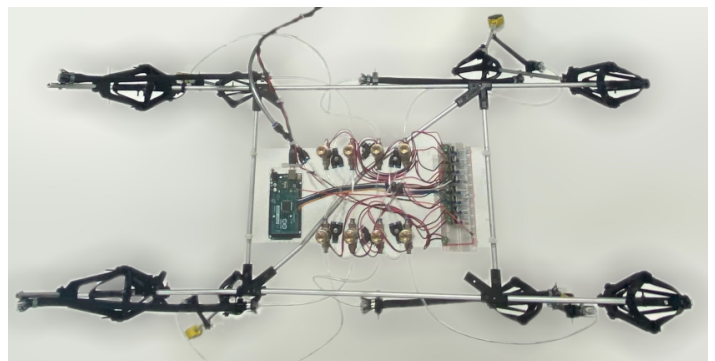
(a) Front view

#### E. Final physical quadruped demonstrator

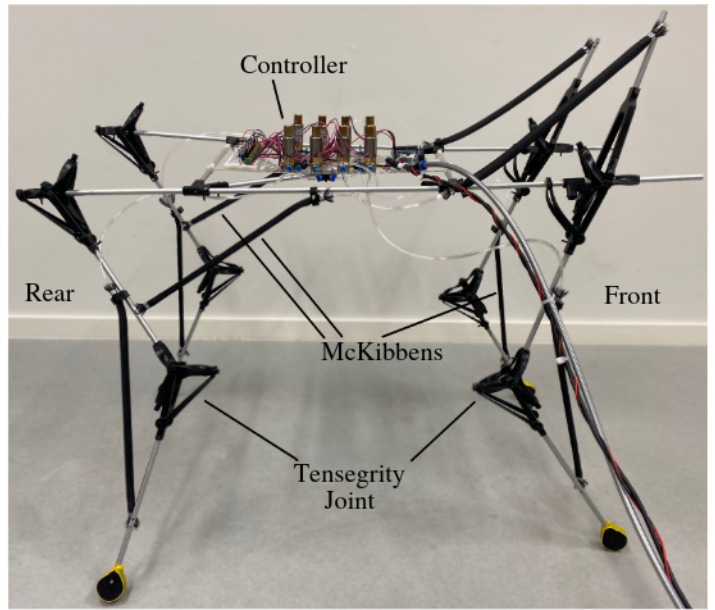
The demonstrator was built using all the calculations, simulations, and measurements conducted prior to this step. The quadruped is an assembly of Ø8mm aluminium rods connected with PETG 3D printed pieces. The pieces are fastened with M3 bolts and nuts. Here is a summary of a few key measurements:

- mass: 3 kg
- dimension: 100cm × 42cm × 84cm
- limb length (hip to knee, knee to feet): 32.6 cm
- working pressure: 3.5 bar (higher pressure cause the valves to leak)
- muscle length: 31 cm

The measurement of the angular change in joint D, from its resting state to actuated state, was approximately 17.87° (see fig 18). This is slightly below the anticipated value of 20°, but the discrepancy, which is 10%, is considered acceptable.



(b) Top view



(c) Side view (right)

Fig. 14: Structure pictures (top view, side view, front view)



Fig. 18: Actuation effect on joint's angle

#### F. Walking Policy

Traditional control methods typically rely on simple PID controllers, or the more efficient MPC, or even Reinforcement Learning. The requirement for the controller is to work with the least amount of sensory feedback as possible. Without precise force or position feedback, it is not practical to implement PID controllers. Moreover, controlling using MPC is out of the question due to the complexity of modelling the non-linear tensegrity joints.

The most feasible option seems to be an open loop controller, with the pace controlled by the small amount of sensory feedback that is available. Designing such sequence can be very tricky since it is easy to fall into making the wrong assumptions about what gait should be used (a diagonal gait, a trotting gait, and much more). The gait that was finally implemented on the demonstrator is described on the figure 19a. The gait that emerged from reinforcement learning training is described on the figure 19b

Reinforcement Learning can help exploring by itself the vast action space. RL can also be influenced toward a particular gait, however, the trained RL was not biased towards any particular gait such that it let emerged the most natural gait for the quadruped topology. Some implementations detail of the RL can be found in the appendix C.

However, the gait emerging from the reinforcement learning did not led to any significant forward speed when tested on

the demonstrator. Only the gait described in fig 19a resulted in forward motion. The figure 16 and 17 illustrate the walking gaits through a series of snapshots.

Randomizing physical parameters (adding random payload, randomizing limb mass, etc.) in the simulator is a good way to take into account the variability of the real world. This help reduces the sim-to-real gap and would eventually lead toward a more robust gait against environmental disturbances (see [11]), it would also induce a less efficient walking gait.

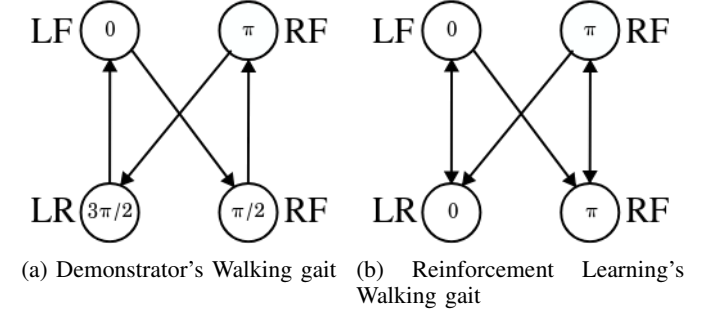


Fig. 19: Walking gaits

#### IV. CONCLUSION

In this work, we presented the design of a quadruped robot platform used to put together tensegrity joints and pneumatic artificial muscles. The final demonstrator robot successfully integrated compliancy in the joints and in the actuators. The quadruped challenges the antagonistic muscle principle by using a combination of restoring force and one McKibben per joint, hence reducing by a factor of two the number of actuators when compared with the antagonistic approach.

The quadruped proved it was able to stand by itself without any active control. The demonstrator also proved the ability to control joints' angle with an onboard controller. Finally, the quadruped topology was demonstrated to be capable of walking with minimal sensory feedback both in simulation and on flat surface with the demonstrator (supported by a rail).

This project is intended to be continued, improving thanks to numerous insights gathered during the simulation and real-



Fig. 16: Walking gait on the demonstrator

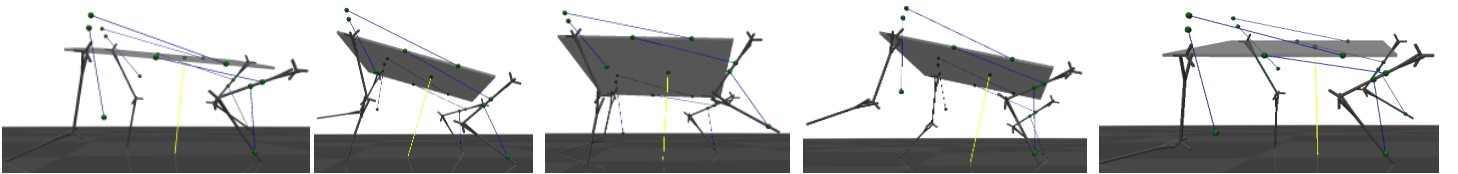


Fig. 17: Walking gait in Mujoco

world testing. The improvement to come can be as well tested using the simulator framework that was used. It is planned to further improve the platform on the following points:

- Design a new tensegrity based joint, with a more selective compliance, and featuring bi-stiffness (joint could be rendered flat for storage or tensioned for nominal usage)
- Design a stronger body (stiffer 3d printed connectors, stiffer rods)
- Bigger feet, increasing the ground friction and the support polygon area
- Implementation of a better walking gait, using Reinforcement Learning with domain randomization to lower the sim-to-reality gap (see [11])

## REFERENCES

- [1] Y. Zhong, R. Wang, H. Feng, and Y. Chen, “Analysis and research of quadruped robot’s legs: A comprehensive review,” *International Journal of Advanced Robotic Systems*, vol. 16, no. 3, p. 172988141984414, May 2019. [Online]. Available: <http://journals.sagepub.com/doi/10.1177/1729881419844148>
- [2] A. Badri-Spröwitz, A. A. Sarvestani, M. Sitti, and Monica A. Daley, “BirdBot achieves energy-efficient gait with minimal control using avian-inspired leg clutching,” *Science Robotics*, vol. 7, no. 64, p. eabg4055, 2022, tex.eprint: <https://www.science.org/doi/pdf/10.1126/scirobotics.abg4055>. [Online]. Available: <https://www.science.org/doi/abs/10.1126/scirobotics.abg4055>
- [3] L. L. Howell, *Introduction to Compliant Mechanisms*. John Wiley Sons, Ltd, 2013, ch. 1, pp. 1–13. [Online]. Available: <https://onlinelibrary.wiley.com/doi/abs/10.1002/9781118516485.ch1>
- [4] M. Hutter, C. Gehring, M. Bloesch, M. Hoepflinger, C. Remy, and R. Siegwart, “StarLETH: a compliant quadrupedal robot for fast, efficient, and versatile locomotion,” Sep. 2012, pp. 483–490.
- [5] T. Boaventura, J. Buchli, C. Semini, and D. G. Caldwell, “Model-based hydraulic impedance control for dynamic robots,” *IEEE Transactions on Robotics*, vol. 31, no. 6, pp. 1324–1336, 2015.
- [6] M. Li, A. Pal, A. Aghakhani, A. Pena-Francesch, and M. Sitti, “Soft actuators for real-world applications,” *Nature Reviews Materials*, vol. 7, no. 3, pp. 235–249, Nov. 2021. [Online]. Available: <https://www.nature.com/articles/s41578-021-00389-7>
- [7] S. Lessard, J. Bruce, E. Jung, M. Teodorescu, V. SunSpiral, and A. Agogino, “A lightweight, multi-axis compliant tensegrity joint,” in *2016 IEEE International Conference on Robotics and Automation (ICRA)*. Stockholm, Sweden: IEEE, May 2016, pp. 630–635. [Online]. Available: <http://ieeexplore.ieee.org/document/7487187/>
- [8] E. Mortensen, “Bio-inspired leg design with adjustable compliance for robot locomotion.”
- [9] K. Narioka, A. Rosendo, A. Spröwitz, and K. Hosoda, “Development of a minimalistic pneumatic quadruped robot for fast locomotion,” in *Proceedings of the 2012 IEEE International Conference on Robotics and Biomimetics (ROBIO), 2012*. Guangzhou: IEEE, 2012, pp. 307–311.
- [10] S. Thomalla and J. Van De Ven, “Modeling and implementation of the mckibben actuator in hydraulic systems,” *IEEE Transactions on Robotics*, vol. 34, no. 6, pp. 1593–1602, Dec. 2018, publisher Copyright: © 2004–2012 IEEE.
- [11] G. Bellegarda, Y. Chen, Z. Liu, and Q. Nguyen, “Robust high-speed running for quadruped robots via deep reinforcement learning,” in *2022 IEEE/RSJ International Conference on Intelligent Robots and Systems (IROS)*, 2022, pp. 10364–10370.

**APPENDIX A**  
**ACTUATORS DRIVER SCHEMATIC**

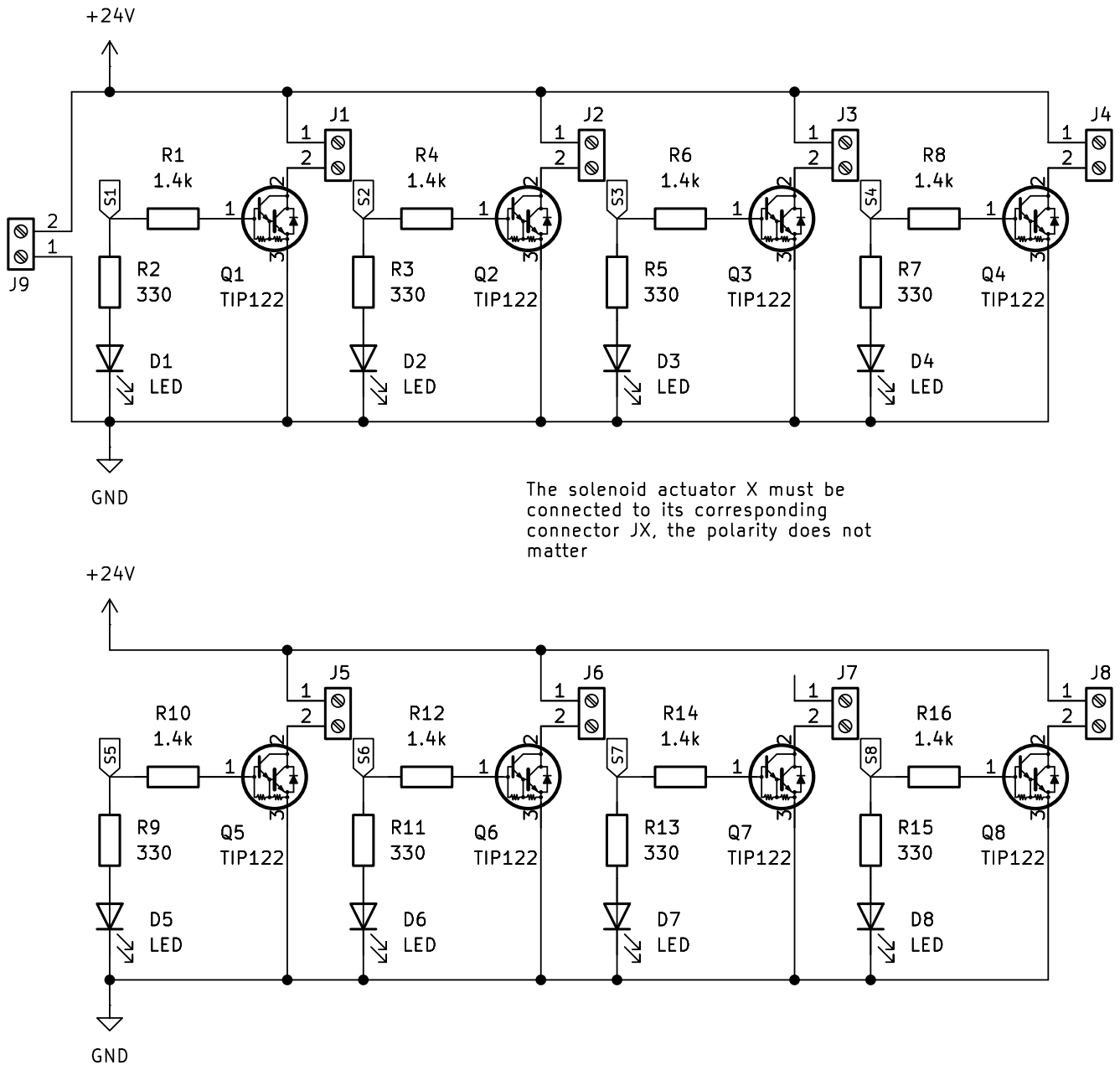


Fig. 20

## APPENDIX B JOINT ITERATIONS

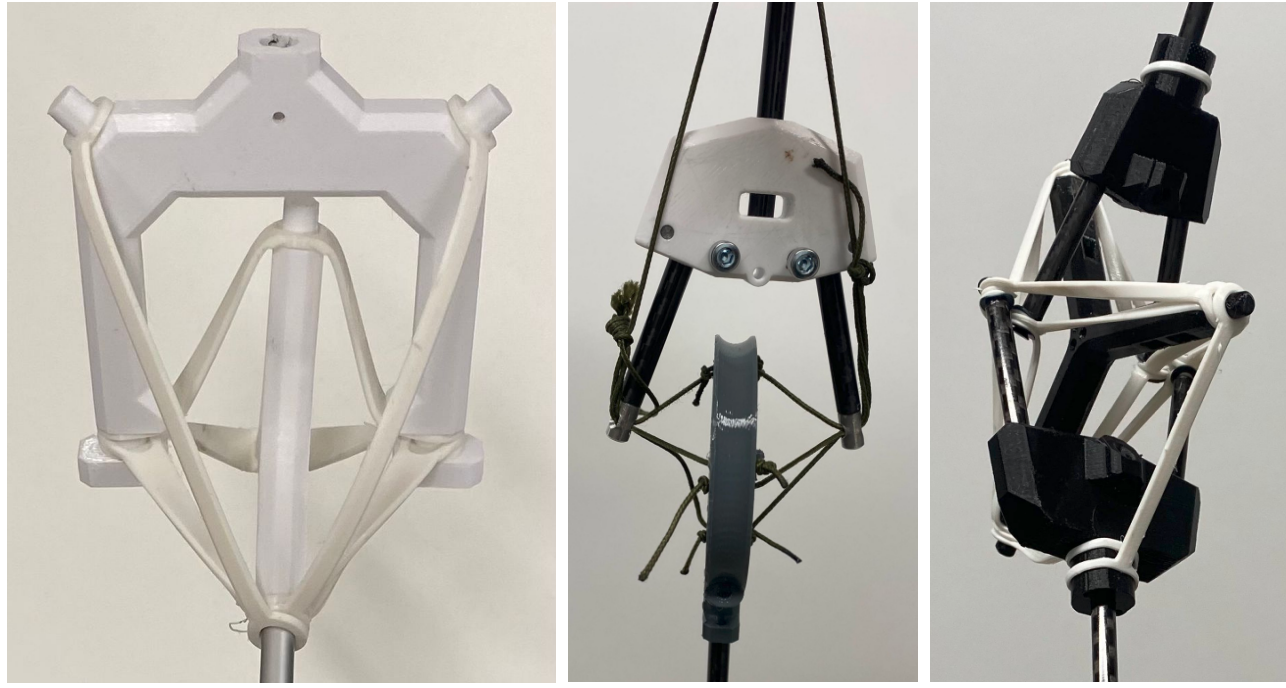


Fig. 21: Some iterations of the tensegrity joints designed throughout the project

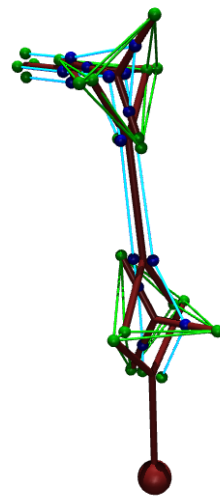


Fig. 22: Tensegrity leg simulated in Mujoco

## APPENDIX C REINFORCEMENT LEARNING

The quadruped learned to walk using reinforcement learning on the simulator Mujoco. OpenAI Gymnasium library was used as a training framework.

- The observation space contains the actuator state, the gravity vector (for roll and pitch), and the linear speed.
- The actuation space contains 8 binary states variables (on/off valve command).
- Network architecture: Multi-Layer Perceptron
- Learning strategy: PPO
- reward function:

$$\begin{aligned}
 & 50 \times v_x + \begin{pmatrix} -1 \\ 0 \\ 0 \end{pmatrix} \cdot \vec{g} \\
 & - 0.0001 \times \left( \sum_i^8 \{\text{actuator state}(t)\}_i + \sum_i^8 \{\text{actuator state}(t) - \text{actuator state}(t-1)\}_i \right) - N_{\text{body colliding with floor, except feet}}
 \end{aligned}$$

## APPENDIX D CODE

All the code produced throughout this project is free and open source, under the *MIT licence*. It is accessible under the public GitHub repository <https://github.com/martantoine/QuadSegrity>